A&A 436, L31–L34 (2005)
DOI: 10.1051/0004-6361:200500117

Astronomy & Astrophysics

Letter to the Editor

INTEGRAL high energy observations of 2S 0114+65

E. W. Bonning[1] and M. Falanga[2]

[1] LUTh, Observatoire de Paris, 92195 Meudon Cedex, France
e-mail: erin.bonning@obspm.fr
[2] CEA Saclay, DSM/DAPNIA/Service d'Astrophysique (CNRS FRE 2591), 91191 Gif-sur-Yvette, France

Received 11 March 2005 / Accepted 28 April 2005

Abstract. We report the first *INTEGRAL* timing and spectral analysis of the high mass X-ray binary source 2S 0114+65 at high energies (5–100 keV). The pulse period was found at 2.668 h with a high pulsed fraction, ~80% in both the 20–40 keV and 40–80 keV energy bands. The spin-up trend over ~8 years was measured to be $\dot{P} = -8.9 \times 10^{-7}$ s s^{-1}. The hard X-ray spectrum obtained with JEM-X/ISGRI is well described by a high energy exponential cut-off power law model where the estimated luminosity is 1.8×10^{36} erg s^{-1} in the 5–100 keV energy band, for a source distance of 7.2 kpc. We tentatively identify a cyclotron resonance scattering feature at ~22 keV with one harmonic, implying a magnetic field of $\sim 2.5 \times 10^{12}$ G.

Key words. pulsars: individual: 2S 0114+65 – stars: neutron – X-rays: stars

1. Introduction

The X-ray source 2S 0114+65 is a high mass X-ray binary (HMXB) consisting of an accreting neutron star (NS) and a type B1a supergiant optical counterpart (LS I+65010) at a distance of ~7.2 kpc (Reig et al. 1996). The pulse period was first measured at 2.78 h (Finley et al. 1992) with a 11.59 day orbital period (Crampton et al. 1985). A spin-up rate over ~11 yr was observed to be $\sim 6.2 \times 10^{-7}$ s s^{-1} (Hall et al. 2000). The long spin period makes this the slowest known X-ray pulsar. Different models have been suggested in the past to explain the peculiar long period pulsation seen in 2S 0114+65 (cf. Hall et al. 2000 and references therein). Most recently, Li & van den Heuvel (1999) suggest that such a slow period is possible if 2S 0114+65 was born as a magnetar with an initial magnetic field strength of $\gtrsim 10^{14}$ G, decaying to a current value of the order 10^{12} G, allowing the NS to spin down to the measured spin period within the lifetime of its companion. The magnetic field has not been measured up to now, as no cyclotron lines have been detected in the X-ray spectrum up to 20 keV. Recently, Farrell et al. (2005) found evidence for a super-orbital period of 30.7 days, suggesting the presence of warped, precessing accretion disk.

Observations by Hall et al. (2000) with *RXTE* show that the 3–20 keV spectrum is best fit by an absorbed power law with exponential high energy cut-off, with photon index ~1.4, cut-off energy ~8 keV, and folding energy ~20 keV, being typical parameters for a HMXB. They find evidence for a fluorescent iron line when the source is in a low emission state, consistent with measurements of Yamauchi et al. (1990).

In this paper, we report the results of high energy *INTEGRAL* observations of 2S 0114+65. The observations are described in Sect. 2. Imaging, timing, and spectral analyses are presented in Sect. 3. A discussion of the results is given in Sect. 4.

2. Observations and data analysis

The present dataset was obtained during the Target of Opportunity (ToO) A02 *INTEGRAL* (Winkler et al. 2003) observation of the Cas A region performed from 5–6 and 7–9 December 2004 (53 345.6–53 346.8 and 53 347.8–53 349.8 MJD), i.e. from part of *INTEGRAL* satellite revolutions 262 and 263. We use data from the coded mask imager IBIS/ISGRI (Ubertini et al. 2003; Lebrun et al. 2003) for a total exposure of 181.9 ks, and from the JEM-X monitor (Lund et al. 2003) for a total exposure time of 11 ks. For ISGRI, the data were extracted for all pointings with a source position offset ≤12°, and for JEM-X with an offset ≤3.5°. The spectrometer (SPI) was not used to extract the hard X-ray spectrum due to the lower sensitivity of this instrument with respect to IBIS/ISGRI for a weak source below 100 keV. Above 100 keV, 2S 0114+65 was neither consistently detected in a single exposure nor in the total exposure time. Data reduction was performed using the standard Offline Science Analysis (OSA) version 4.2 (Courvoisier et al. 2003). The background subtracted ISGRI light curve for the timing analysis was reduced using dedicated software *ii_light_extract* (version to be included in OSA 5.0). The ISGRI light curve per energy band was obtained for each 300 s long time bin.

3. Results

3.1. ISGRI imaging

Figure 1 shows a significance map around the source 2S 0114+65 in the 20–40 keV energy range. Single

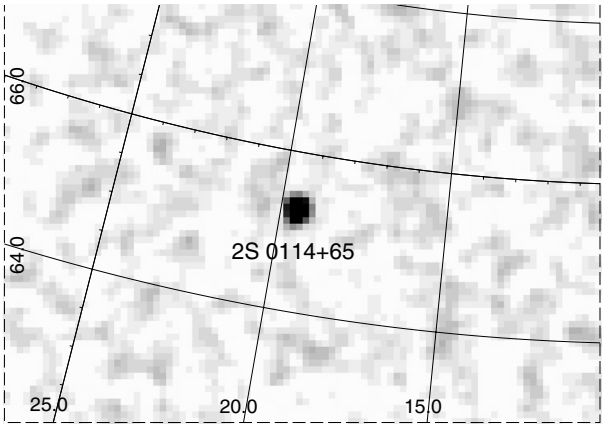

Fig. 1. The 20–40 keV IBIS/ISGRI mosaicked and deconvolved sky image of the ~182 ks observation. Image size is ~15° × 5°, centered at 2S 0114+65 position. The pixel size is 5′. 2S 0114+65 was detected at a significance of ~37σ.

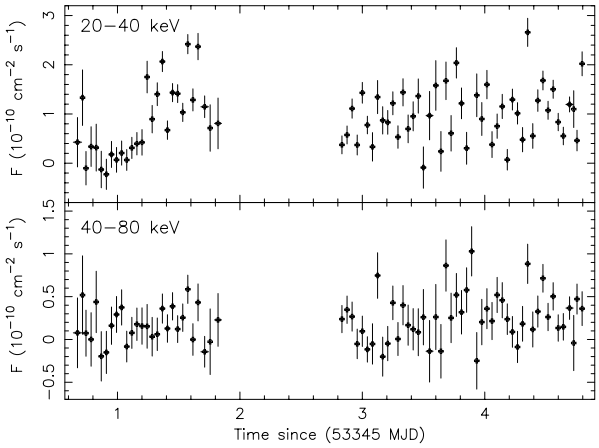

Fig. 2. *INTEGRAL*/ISGRI light curve of 2S 0114+65 in the 20–40 and 40–80 keV energy bands. The ISGRI data are taken from the whole observation and have been converted to flux assuming a power law with an exponential high-energy cut-off model (see Table 1). Each point corresponds to a ~2.2 ks interval.

pointings were deconvolved and analyzed separately, and then combined in mosaic images. The source is clearly detected at a significance level of 36.6σ. In the energy range 40–80 keV, the significance level was 10.8σ. From the ISGRI data, 2S 0114+65 was observed with the imaging procedure at the position α_{J2000} = 01^{h}18^{m}02^{s}.55 and δ_{J2000} = 65°17′02″.3. The source position offset with respect to the catalog position (Bradt & McClintock 1983) is 0.5′. This is within the 90% confidence level assuming the imaging source location error given by Gros et al. (2003).

3.2. Timing analysis

The ISGRI 20–40 keV and 40–80 keV high energy light curves were extracted from the images using all available pointings and are shown in Fig. 2. During the first ~30 ks of the observation, the flux rises to a mean count rate in the 20–40 keV energy band of ~1.6 cts s^{-1} (~9.5×10^{-11} erg s^{-1} cm^{-2}). Similarly, but less significantly, the flux in the 40–80 keV energy bands attains a count rate of ~0.5 cts s^{-1} (~2.6×10^{-11} erg s^{-1} cm^{-2}). The count rate is converted to flux assuming a power law with an exponential high-energy cut-off power-law model (see Table 1, Sect. 3.3). The hardness ratio of these energy bands as a function of time indicates that no significant spectral variability was detected.

We searched for coherent pulsations of the source in the 20–40 keV energy band where we have the best statistics. Using the 300 s binned light curve of the source in the 20–40 keV energy band, we computed a Power Density Spectrum (PDS) in the frequency range between 6.5×10^{-6} and 1.6×10^{-3} Hz from Fast Fourier Transforms. In the resulting PDS, an evident signal is present at $\nu = 1.04 \times 10^{-4}$ Hz. The highest peak in the power spectrum corresponds to a nominal period of 2.67 h. The accurate period was found using the phase-delay fitting method. We divided the data over 8 intervals of ~23 ks each and folded the light curve corresponding to each of the intervals using the nominal pulse period. The pulse period was not significantly detected in the first interval.

Table 1. Spectral best fit parameters.

Dataset	JEM-X/ISGRI
model	PL × HIGHECUT
Γ	$1.6^{+0.5}_{-0.5}$
E_{cut} (keV)	$9.0^{+14.1}_{-8.8}$
E_{fold} (keV)	$22.1^{+12.1}_{-6.0}$
χ^2/d.o.f.	14.5/15
L_{5-100} keV (erg s^{-1})	1.8×10^{36}

Hall et al. (2000) suggest that 2S 0114+65 is an eclipsing system, which may explain the very low source flux in this first interval. However, using their ephemeris, the orbital period 11.63 ± 0.007 days given by Corbet et al. (1999), and no orbital period evolution, we find the region of low flux in our observation to lie directly within the error of the expected location of the eclipse. For intervals 2–8, we found the pulse phase delays of each of the folded light curves with respect to the second interval. We fitted these phase delays with the first two terms of the equation $\delta\phi = \delta\phi_\circ + \delta\omega(t - t_\circ) + \frac{1}{2}\dot{\omega}(t - t_\circ)^2$, where $\delta\phi$ is the measured pulse phase delay, $t_\circ$ is the mid time of the observation, $\delta\phi_\circ$ is the phase delay at $t_\circ$, $\delta\omega$ is the deviation from the nominal pulse frequency, and $\dot{\omega}$ is the pulse frequency derivative. The best determination of the mean pulse period was found to be P = 2.668 ± 0.004 h. Errors are at 1σ confidence level. The short observation time and low statistics did not allow us to determine or give an upper limit on the pulse derivative.

The folded light curve (excluding the first interval where the pulse period was not detected above 3σ) is shown in Fig. 3. The pulse profiles show a single peak up to 80 keV similar to that observed previously at lower energies, cf. Hall et al. (2000) and Corbet et al. (1999). The pulsed fraction (PF), defined here as PF = $(I_{max} - I_{min})/(I_{max} + I_{min})$, is measured at 76 ± 5% in the 20–40 keV energy range and 84 ± 20% in the 40–80 keV band.

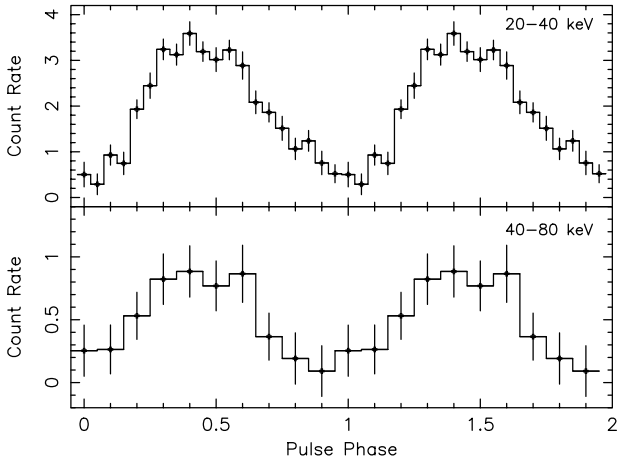

Fig. 3. IBIS/ISGRI background subtracted light curve of 2S 0114+65 folded at the best found NS spin period (2.668 h). The epoch T_0 is arbitrary. From top to bottom the energy ranges are 20–40 keV and 40–80 keV, respectively. The pulse profile is repeated once for clarity.

3.3. Spectral analysis

The spectral analysis was done using XSPEC version 11.3 (Arnaud 1996), combining the 20–100 keV ISGRI data with the simultaneous 5–20 keV JEM-X data. Due to the short exposure time of JEM-X, and therefore lower statistics, we rebinned this data in a 5 channel energy response matrix in order to constrain the ISGRI spectrum at higher energy. For ISGRI we used a 15 channel energy response matrix. A constant factor was included in the fit to take into account the uncertainty in the cross-calibration of the instruments. The factor was fixed at 1 for the ISGRI data. A systematic error of 2% was applied to the JEM-X/ISGRI spectra which corresponds to the current uncertainty in the response matrix. All spectral uncertainties in the results are given at a 90% confidence level for single parameters.

The joint JEM-X/ISGRI (5–100 keV) spectrum was first fitted with a simple model consisting of a power law, which was found inadequate with χ^2/d.o.f. = 49.5/17. In order to compare with previously reported measurements (Hall et al. 2000), we fit a common model for HMXBs, namely a power law with exponential high energy cut-off. The photon flux density adopts the form $f(E) = AE^{-\Gamma}e^{(E_{\rm cut}-E)/E_{\rm fold}}$, where A is a normalization constant. This model gives a better fit with χ^2/d.o.f. = 14.5/15, and the resulting best fit parameters $\Gamma = 1.6$, $E_{\rm cut} = 9.0$ keV and $E_{\rm fold} = 22.1$ keV, are consistent within their errors with the previously published values of Hall et al. (2000).

We note that there is a feature in the residuals to this fit (see Fig. 5) around 40–50 keV. This is suggestive of a cyclotron resonance scattering feature (CRSF), which is observed in many accreting X-ray pulsars (Coburn et al. 2002) at high energies. We attempted to test the hypothesis of a cyclotron feature in the spectrum by modifying the power-law model with a two-harmonic cyclotron absorption line (Mihara et al. 1990). This fit shows a CRSF at 22 keV with a first harmonic at 44 keV and line widths 9.8 and 1.7 keV respectively. Although this model removes the dip feature in the residuals, the χ^2/d.o.f. of 5.4/10 does not improve the fit.

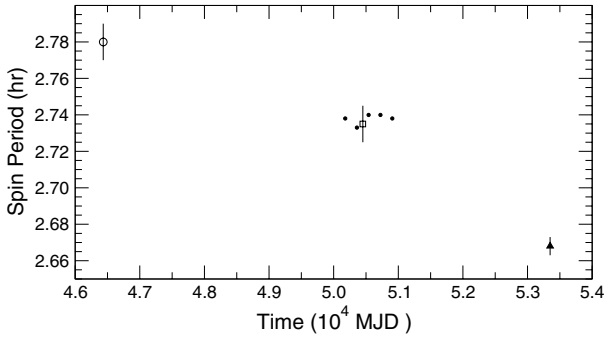

Fig. 4. Spin history of 2S 0114+65. The filled triangle is from this work. The open circle is from Finley et al. (1992), filled circles from Corbet et al. (1999), and open square from Hall et al. (2000).

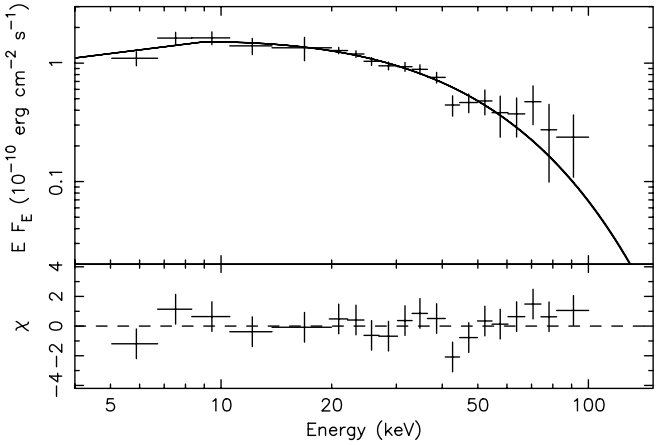

Fig. 5. *INTEGRAL*/JEM-X (5–20 keV) and ISGRI (20–100 keV) unfolded spectra of 2S 0114+65 with the best-fit power law and exponential high-energy cut-off model. Residuals between the data and model are shown in the bottom panel in units of sigma.

Absorption by neutral hydrogen was not included in these models since previous reported values of the hydrogen column density, $\sim 3 \times 10^{22}$ cm^{-2} (Hall et al. 2000) did not have effects above 5 keV. Similarly to the timing analysis, we excluded the first 14 pointings of the total ISGRI spectrum. The best fit parameters of the model together with their errors are reported in Table 1. The flux was converted to luminosity assuming a distance of 7.2 kpc (Reig et al. 1996). The fairly large errors reported for the best fit parameters $E_{\rm cut}$ and the related $E_{\rm fold}$ are substantially due to the low statistics of the JEM-X data. The unfolded spectrum and the residuals of the data are shown in Fig. 5.

4. Conclusions

We have carried out a temporal and spectral analysis for the first time with *INTEGRAL* data of the HMXB 2S 0114+65. We determined the spin period to be 2.668 h, which indicates that the long-term spin-up of the NS is still continuing. In Fig. 4, we show the detailed pulse period history of the source from the first determination in 1986 with *EXOSAT*. Since 1996, the spin period has decreased from ~2.73 h to ~2.67 h. The measured spin period derivative from MJD 50451 to MJD 53348 is $\dot{P} = -8.9 \times 10^{-7}$ s s^{-1} which is ~1.4 times as large as the value

Article published by EDP Sciences and available at http://www.edpsciences.org/aa or http://dx.doi.org/10.1051/0004-6361:200500117

reported by Hall et al. (2000). The increase in $\dot{P}$ likely occurs from an increase of accreting matter, and shows that the spin-up is not a linear trend. The pulsed fraction is observed to be significant up to 80 keV, 76% in the range 20–40 keV and 84% in the range 40–80 keV. The detection of pulsed emission up to 80 keV and the measured spin-up trend strongly support the conclusion that 2S 0114+65 is a rotating neutron star where the pulsed photons arise from the polar cap on the NS surface.

The energy spectrum of 2S 0114+65 from 5–100 keV is well fit by the standard model used for X-ray binary pulsars, i.e. a power law with exponential high energy cut-off. Best fit parameters give a photon index 1.6, cut-off energy 9.0 keV, and folding energy 22.1 keV. The X-ray luminosity calculated from the model flux is 1.8×10^{36} erg s^{-1} from 5–100 keV, assuming the source distance to be 7.2 kpc.

If the presence of a cyclotron resonance scattering feature with $E_{\rm cyc} \sim 22$ keV is confirmed, the magnetic field will be $\sim 2.5 \times 10^{12}$ G, assuming a 1.4 $M_{\odot}$ NS with a radius of 10 km and scattering in the accretion column region above the polar cap on the NS surface. The magnetic field of the NS is given by $E_{\rm cyc} = 11.6\, B_{12}\, (1+z)^{-1}$ keV, where B_{12} is the magnetic field in units of 10^{12} G, and $(1+z)$ is the gravitational redshift. This value is consistent for X-ray pulsars with cut-off energies around 10 keV. Unfortunately, the statistics of the high energy data (with our exposure time) prevent us from confirming the existence of the CRSF. More extensive *INTEGRAL* observations at high energy should allow this result to be tested with a longer exposure time.

Acknowledgements. E.B. is a Chateaubriand Fellow at the Observatory of Paris. M.F. acknowledges the French Space Agency and CNRS for financial support. The authors are grateful to A. Gros and S. Chazalmartin for providing the light curve software.

References

Arnaud, K. A. 1996, in ASP Conf. Ser., 101, 17
Bradt, H. V. D., & McClintock, J. E. 1983, ARA&A, 21, 13
Coburn, W., Heindl, W. A., Rothschild, R. E., et al. 2002, ApJ, 580, 394
Corbet, R. H. D., Finley, J. P., & Peele, A. G. 1999, ApJ, 511, 876
Courvoisier, T. J.-L., Walter, R., Beckmann, V., et al. 2003, A&A, 411, L53
Crampton, D., Hutchings, J. B., & Cowley, A. P. 1985, ApJ, 299, 839
Farrell, S. A., Sood, R. K., & O'Neill, P. M. 2005, MNRAS, submitted [arXiv:astro-ph/0502008]
Finley, J. P., Belloni, T., & Cassinelli, J. P. 1992, A&A, 262, L25
Gros, A., Goldwurm, A., Cadolle-Bel, M., et al. 2003, A&A, 411, L179
Hall, T. A., Finley, J. P., Corbet, R. H. D., & Thomas, R. C. 2000, ApJ, 536, 450
Lebrun, F., Leray, J. P., Lavocat, P., et al. 2003, A&A, 411, L141
Li, X.-D., & van den Heuvel, E. P. J. 1999, ApJ, 513, L45
Lund, N., Budtz-Jørgensen, C., Westergaard, N. J., et al. 2003, A&A, 411, L231
Mihara, T., Makishima, K., Ohashi, T., Sakao, T., & Tashiro, M. 1990, Nature, 346, 250
Reig, P., Chakrabarty, D., Coe, M. J., et al. 1996, A&A, 311, 879
Ubertini, P., Lebrun, F., Di Cocco, G., et al. 2003, A&A, 411, L131
Winkler, C., Courvoisier, T. J.-L., Di Cocco, G., et al. 2003, A&A, 411, L1
Yamauchi, S., Asaoka, I., Kawada, M., Koyama, K., & Tawara, Y. 1990, PASJ, 42, L53